

A complete NLO calculation of the J/ψ and ψ' production at hadron colliders*

Yan-Qing Ma and Kai Wang

Department of Physics and State Key Laboratory of Nuclear Physics and Technology, Peking University, Beijing 100871, China

Kuang-Ta Chao

*Department of Physics and State Key Laboratory of Nuclear Physics and Technology,
and Center for High Energy Physics, Peking University, Beijing 100871, China*

(Dated: October 27, 2011)

A complete next-to-leading order (NLO) calculation in α_s for the J/ψ and ψ' prompt production at the Tevatron, LHC, and RHIC in nonrelativistic QCD is presented. We argue that the next-to-next-to-leading order (NNLO) color-singlet contribution may not be so important as to resolve the large discrepancy between theory and experiment in J/ψ large p_T production cross sections. Therefore, a complete NLO calculation, including both color-singlet and color-octet contribution, is necessary and essential to give a good description for J/ψ and ψ' production. We also study the methods to fit the long-distance matrix elements using either two linear combined matrix elements or three matrix elements, and find these two methods can give consistent results. Compared with the measurements at the LHC and RHIC for prompt J/ψ and ψ' production, our predictions are found to agree with all data. In particular, the recently released large p_T data (up to 60-70 GeV) at the LHC are in good agreement with our predictions. Our results imply that the universality of color-octet matrix elements holds approximately in charmonium hadroproduction, when one uses fixed order perturbative calculation to describe data (the data in small p_T region are not included). Our work may provide a new test for the universality of color-octet matrix elements, and the color-octet mechanism in general.

PACS numbers: 12.38.Bx, 13.85.Ni, 14.40.Pq

I. INTRODUCTION

Heavy quarkonium is a multiscale system which can probe various regimes of QCD. Thus, an understanding of heavy quarkonium production is particularly interesting. To solve the large discrepancy between CDF data at the Fermilab Tevatron[2] of ψ' production at high p_T and theoretical predictions, the color-octet (CO) mechanism [3] was proposed based on nonrelativistic QCD (NRQCD) factorization[4]. With the CO mechanism, $Q\bar{Q}$ pairs can be produced at short distances in CO ($^1S_0^{[8]}$, $^3S_1^{[8]}$, $^3P_J^{[8]}$) states and subsequently evolve into physical quarkonia by nonperturbative emission of soft gluons. It can be verified that the partonic differential cross sections at leading-order (LO) in α_s behave as $1/p_T^4$ for $^3S_1^{[8]}$, and $1/p_T^6$ for $^1S_0^{[8]}$ and $^3P_J^{[8]}$, all of which decrease at high p_T much slower than $1/p_T^8$ of the color-singlet (CS) state. The CO mechanism could give a natural explanation for the observed p_T distributions and large production rates of ψ' and J/ψ [5, 6]. However, CO mechanism seems to encounter difficulties when the polarization of J/ψ is also taken into consideration [7, 8]. To exploit the underlying physics, lots of efforts have been made, either by introducing new channels[9–11] or by proposing other mechanisms[12, 13].

It is a significant step to work out the next-to-leading order (NLO) QCD correction for the CS channel, which enhances the differential cross section by about 2 orders of magnitude at high p_T [14], and changes the J/ψ polarization from being transverse at LO into longitudinal at NLO[15]. Although the CS NLO cross section still lies far below the experimental data, it implies that, compared to the α_s suppression, kinematic enhancement at high p_T is more important in the current issue. This observation is also supported by our recent work[16] for χ_c production, where we find the ratio of production rates of $\sigma_{\chi_{c2}}/\sigma_{\chi_{c1}}$ can be dramatically altered by the NLO contribution due to change of the p_T distribution from $1/p_T^6$ at LO to $1/p_T^4$ at NLO in the CS P-wave channels. So we can conclude nothing definite until all important channels in $1/p_T$ expansion are presented. It means the CO channels $^1S_0^{[8]}$ [18] and $^3P_J^{[8]}$ should be considered at NLO, while the CS channel $^3S_1^{[1]}$ at next-to-next-to-leading order (NNLO) in α_s . Among these corrections, the complete NNLO calculation for the CS channel is currently beyond the state of the art, and instead, the NNLO* method is proposed[19, 20]. Compared to NLO, the only potentially not suppressed contribution within NNLO CS channel is gluon fragmentation, which gives a new scaling behavior of $1/p_T^4$ for the cross section. But, as studied in ref.[21], these fragmentation contributions are ignorable, compared with experimental prompt production data of J/ψ , and we will further argue about this point in Sec. III A. As a result, we expect a complete NLO calcula-

*An expanded version based on Ref.[1].

\sqrt{S} (TeV)	region of y	r_0	r_1
1.96	(0 , 0.6)	3.9	-0.56
7	(0 , 0.75)	4.0	-0.55
7	(0.75, 1.50)	3.9	-0.56
7	(1.50, 2.25)	3.9	-0.59
7	(0 , 2.4)	4.1	-0.56
7	(0 , 1.2)	4.1	-0.55
7	(1.2, 1.6)	3.9	-0.57
7	(1.6, 2.4)	3.9	-0.59
7	(2.5, 4)	3.9	-0.66
7	(2 , 2.5)	4.0	-0.61
7	(2.5, 3)	4.0	-0.65
7	(3 , 3.5)	4.0	-0.68
7	(3.5, 4)	4.0	-0.74
7	(4 , 4.5)	4.2	-0.81
14	(0 , 3)	3.9	-0.57
0.2	(0 , 0.35)	3.8	-0.60
0.2	(1.2 , 2.4)	4.0	-0.66

TABLE I: Experimental conditions with various experimental collaborations. r_0 and r_1 are theoretical predictions related to the short-distance coefficients.

tion of J/ψ production is necessary and sufficient to give a reasonable description of the experiment data.

Currently, while J/ψ production in two-photon collisions at CERN LEP2[22] and photoproduction at DESY HERA[23–25] are shown to favor the presence of CO contribution, the J/ψ production at B factories is described well using NLO CS model and leaves little room for the CO contributions[26–29]. J/ψ production in association with a W -boson or Z^0 -boson at the LHC is also studied [30]. However, in all previous works for heavy quarkonium production, CO long-distance matrix elements (LDMEs) were extracted at LO, which suffer from large uncertainties. In order to further test the CO mechanism, it is necessary to extract CO LDMEs at NLO level. This was studied in our recent work Ref.[16] for χ_{cJ} and Refs.[1, 17] for J/ψ and ψ' . Based on Ref.[1], we further study J/ψ and ψ' hadron production including more detailed discussions in this work.

The remainder of this paper is organized as follows. In Sec. II, we perform a fit to the CO LDMEs for ψ' and J/ψ using the p_T distributions measured by CDF in Ref.[31] and Ref.[32] respectively. In the fit of J/ψ , feed-down contributions from χ_{cJ} and ψ' are considered. We refer interested readers to Ref.[17] for details on the calculation and the input parameters. We will study further theoretical uncertainties in Sec. III. Then, we compare our predictions with new LHC data and RHIC data in Sec.V. After that, a related work of NLO correction to J/ψ production is compared with ours. We finally give a brief summary in Sec. VI.

II. FIT COLOR-OCTET MATRIX ELEMENTS

We find $^3P_J^{[8]}$ channels have a large K factor and can give important contributions, thus the $^3S_1^{[8]}$ channel is no

H	$\langle \mathcal{O}^H \rangle$ (GeV ³)	M_{1,r_1}^H (10 ⁻² GeV ³)	M_{0,r_0}^H (10 ⁻² GeV ³)
J/ψ	1.16	$0.05 \pm 0.02 \pm 0.02$	$7.4 \pm 1.9 \pm 0.4$
ψ'	0.76	$0.12 \pm 0.03 \pm 0.01$	$2.0 \pm 0.6 \pm 0.2$

TABLE II: Fitted Color-Octet LDMEs in $J/\psi(\psi')$ production with $p_T^{\text{cut}} = 7$ GeV. Here $r_0 = 3.9$, $r_1 = -0.56$ are determined from short-distance coefficient decomposition at Tevatron. The first errors are due to renormalization and factorization scale dependence, while the second errors come from the fit. Color-Singlet ($^3S_1^{[1]}$) LDMEs $\langle \mathcal{O}^H \rangle$ are estimated using a potential model result[33].

longer the unique source for the high p_T contribution. In fact, the following decomposition for the short-distance coefficients holds within an error of a few percent:

$$d\hat{\sigma}[^3P_J^{[8]}] = r_0 d\hat{\sigma}[^1S_0^{[8]}] + r_1 d\hat{\sigma}[^3S_1^{[8]}], \quad (1)$$

where we find $r_0 = 3.9$ and $r_1 = -0.56$ for the experimental condition with CDF at the Tevatron. $r_{0,1}$ for other conditions discussed in this work can be found in Table I. As a result, it is convenient to use two linearly combined LDMEs

$$\begin{aligned} M_{0,r_0}^{J/\psi} &= \langle \mathcal{O}^{J/\psi}(^1S_0^{[8]}) \rangle + \frac{r_0}{m_c^2} \langle \mathcal{O}^{J/\psi}(^3P_0^{[8]}) \rangle, \\ M_{1,r_1}^{J/\psi} &= \langle \mathcal{O}^{J/\psi}(^3S_1^{[8]}) \rangle + \frac{r_1}{m_c^2} \langle \mathcal{O}^{J/\psi}(^3P_0^{[8]}) \rangle, \end{aligned} \quad (2)$$

when comparing theoretical predictions with experimental data for production rates at the Tevatron and LHC. As pointed out in Ref. [17], although both $\langle \mathcal{O}^{J/\psi}(^3S_1^{[8]}) \rangle$ and $d\hat{\sigma}[^3P_J^{[8]}]$ depend on the renormalization scheme and the renormalization scale μ_Λ , $M_{1,r_1}^{J/\psi}$ is almost independent of them.

We note that the curvature of experimental cross section is positive at large p_T but negative at small p_T , with a turning point at $p_T \approx 6$ GeV. But the theoretical curvature is always positive. This implies that data below 7 GeV can not be well explained in fixed order perturbative QCD calculations. If including these data in the fit, it will cause a large χ^2 , which indicates the fit is not reliable. Therefore, in our fit we introduce a p_T^{cut} and only use experimental data for the region $p_T \geq p_T^{\text{cut}}$. In the following we use $p_T^{\text{cut}} = 7$ GeV.

By fitting the p_T distributions of prompt ψ' and J/ψ production measured at the Tevatron[31, 32] in Fig. 1 and Fig. 2, the CO LDMEs are determined as showing in Table II, while the CS LDMEs are estimated using a potential model result of the wavefunctions at the origin[33]. In Fig. 1 and Fig. 2 we also give the predictions of prompt ψ' and J/ψ production at LHC with $\sqrt{S} = 14$ TeV and $|y| < 3$.

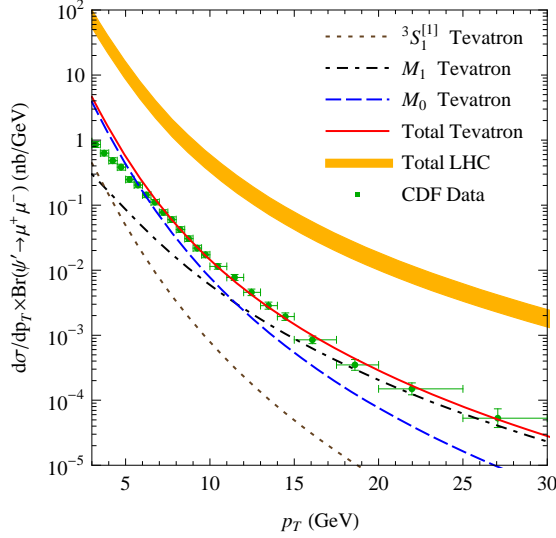


FIG. 1: (Color online.) Transverse momentum distributions of prompt ψ' production at the Tevatron and LHC. CDF data are taken from Ref.[31]. The LHC prediction corresponds to $\sqrt{S} = 14$ TeV and $|y_{J/\psi}| < 3$.

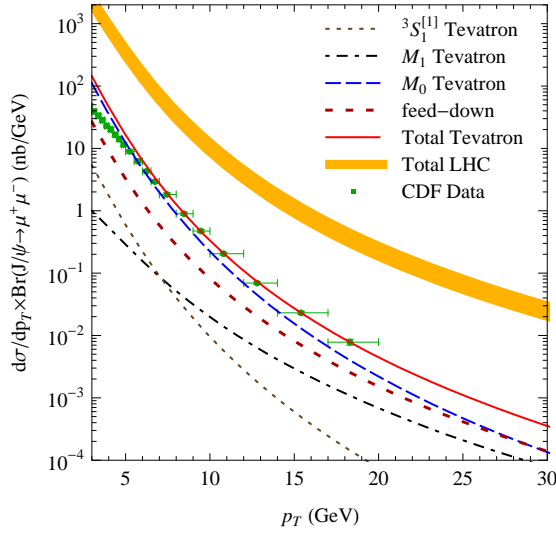


FIG. 2: (Color online.) Transverse momentum distributions of prompt J/ψ production at the Tevatron and LHC. CDF data are taken from Ref.[32]. The LHC prediction corresponds to $\sqrt{S} = 14$ TeV and $|y_{\psi'}| < 3$.

III. THEORETIC UNCERTAINTIES

A. Uncertainty from NNLO color-singlet contribution

Ordinarily, errors come from higher order contributions can be estimated by varying renormalization scale and factorization scale. This is the case for CO contribu-

tions which have been considered in the fit. However, for CS contribution, new kinematic enhanced channels will open at NNLO which behavior as $1/p_T^4$. Because the new channels have different p_T behavior from LO and NLO contributions, its influence can not be simply estimated just by varying parameters at NLO calculation.

A complete NNLO calculation for CS is currently far beyond the state of the art, instead, a NNLO* method is proposed[19, 20], in which only tree level diagrams are considered and an infrared cutoff (s_{ij}^{\min}) is imposed to control soft and collinear divergences. As $1/p_T^4$ behavior channels are presented for the first time at NNLO, their contributions do not have divergences and should almost not dependent on s_{ij}^{\min} supposing s_{ij}^{\min} is sufficiently small. Generally, for small s_{ij}^{\min} and large p_T , the NNLO* contributions can be expanded as

$$d\sigma_{\text{NNLO}^*} = c_4 \frac{1}{p_T^4} + c_6 \frac{\log^2(p_T^2/s_{ij}^{\min})}{p_T^6} + \dots, \quad (3)$$

where ... represents remained contributions which are not important. To demonstrate terms other than $1/p_T^4$ have negligible contributions, authors in Ref. [19] vary the s_{ij}^{\min} and show that the yield $d\sigma_{\text{NNLO}^*}$ becomes insensitive to the value of s_{ij}^{\min} as p_T increases. The NNLO* contributions are then concluded to be large and important[19, 20].

In the following, however, we will argue that the NNLO CS contribution should not be so large as the NNLO* method expected. We first point out that, there could be a misunderstanding in Ref. [19] when trying to demonstrate the $1/p_T^4$ term is the most important one. In fact, even if the second term in Eq. (3) is much larger than the first term, $d\sigma_{\text{NNLO}^*}$ will also become insensitive to s_{ij}^{\min} at large p_T , the reason is

$$\frac{\log^2(p_T^2/s_{ij}^{\min})}{\log^2(p_T^2/s_{ij}^{\prime\prime\min})} \rightarrow 1, \text{ as } p_T \rightarrow \infty. \quad (4)$$

Thus it is needed to restudy which term is dominant in $d\sigma_{\text{NNLO}^*}$ in the current experimental p_T region.

Our strategy to study this problem is fitting the p_T behavior of

$$R^* = d\sigma_{\text{NNLO}^*}/d\sigma_{\text{NLO}}, \quad (5)$$

where $d\sigma_{\text{NLO}}$ is well known to behave as $1/p_T^6$ at large p_T . If c_4 term is dominant in $d\sigma_{\text{NNLO}^*}$, R^* will behave as p_T^2 ; while if c_6 term is dominant, R^* will behave as $\log^2(p_T^2/s_{ij}^{\min})$. As there is no difference between J/ψ and Υ except a mass scale change, we will use the $d\sigma_{\text{NNLO}^*}$ results for Υ in Ref. [19]. Specifically, we define

$$f_1 = \frac{R^*}{p_T^2} \Big|_{s_{ij}^{\min}=0.5m_b^2},$$

$$f_2 = \frac{R^*}{\log^2(p_T^2/s_{ij}^{\min})} \Big|_{s_{ij}^{\min}=0.5m_b^2}, \quad (6)$$

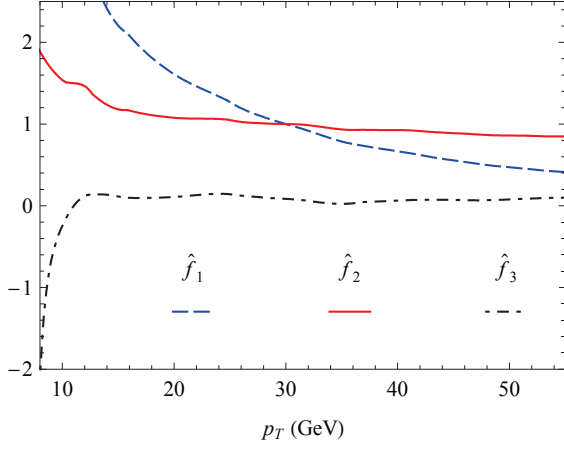


FIG. 3: (Color online.) Transverse momentum distributions of functions of \hat{f}_1 , \hat{f}_2 and \hat{f}_3 . It implies the NNLO^{*} result is dominated by the double logarithm enhancement, which will be canceled in a complete NNLO calculation. See text for definition of \hat{f}_i .

while \hat{f}_1 and \hat{f}_2 correspond to f_1 and f_2 normalized at $p_T = 30$ GeV. The transverse momentum distributions of \hat{f}_1 and \hat{f}_2 are presented in Fig. 3, where we find \hat{f}_2 is almost fixed to 1 when $p_T > 15$ GeV while \hat{f}_1 still varies significantly in this p_T region. As a result, the R^* behaves similar to $\log^2(p_T^2/s_{ij}^{\min})$. To further test this double logarithm behavior, we define

$$\hat{f}_3 = 1 - \frac{R^*/\log^2(p_T^2/s_{ij}^{\min})|_{s_{ij}^{\min}=2m_b^2}}{R^*/\log^2(p_T^2/s_{ij}^{\min})|_{s_{ij}^{\min}=0.5m_b^2}}. \quad (7)$$

It can be found in Fig. 3 that \hat{f}_3 is very close to 0 when $p_T > 12$ GeV, which confirms our expectation for the double logarithm behavior.

Based on the above discussion, we may conclude that $d\sigma_{\text{NNLO}^*}$ in the current experimental p_T region is dominated by c_6 term which has double logarithm enhancement relative to NLO result¹. The double logarithm, originated from IR cutoff, will be canceled in a complete NNLO calculation with both real and virtual corrections taken into consideration. Therefore, a complete NNLO result should have no large enhancement relative to NLO result[17], considering the suppression due to an extra α_s in NNLO. In other words, the NNLO^{*} method may have overestimated the NNLO contributions.

Having found that the NNLO CS contribution should not be large relative to the NLO contribution, we may ignore the theoretical uncertainty from NNLO because the CS NLO result is smaller than experimental data by at least a factor of 10 at $p_T > 7$ GeV.

¹ We have not considered the $\frac{\log^4(p_T^2/s_{ij}^{\min})}{p_T^2}$ term in the expansion in Eq. 3, which is important in the region of $p_T^2 \gtrsim s_{ij}^{\min}$.

B. Uncertainty from decomposing P-wave channels

There are two reasons that we should further consider the decomposed P-wave channel. One is the decomposition in Eq.(1) is not exact, although it holds within a few percent, hence we need to study whether this small error will be enlarged when comparing with experimental data. The other reason is that r_0 and r_1 vary with different center-of-mass energies or different experimental cuts introduced in experiments, thus the two LDMEs M_{0,r_0}^H and M_{1,r_1}^H cannot be universally used. Regarding this point, we find the changes of r_0 and r_1 are not large in different cases (see Table I). As a result, M_{0,r_0}^H and M_{1,r_1}^H extracted from the CDF data can be approximately used to predict other experimental results. But this can also cause some errors. A convenient method to cover all these theoretical uncertainties is fitting the experimental data using three independent LDMEs. As pointed out above, data with $p_T < 7$ GeV may not be well explained by the fixed order perturbative QCD calculations, so in the fit we still choose $p_T^{\text{cut}} = 7$ GeV, which is safer for the application of perturbative QCD.

For the J/ψ , by minimizing χ^2 , we get

$$\begin{aligned} O_1 &\equiv \langle \mathcal{O}^{J/\psi}(^1S_0^{[8]}) \rangle = 15.7 \times 10^{-2} \text{ GeV}^3 (\pm 129\%), \\ O_2 &\equiv \langle \mathcal{O}^{J/\psi}(^3S_1^{[8]}) \rangle = -1.18 \times 10^{-2} \text{ GeV}^3 (\pm 249\%), \quad (8) \\ O_3 &\equiv \frac{\langle \mathcal{O}^{J/\psi}(^3P_0^{[8]}) \rangle}{m_c^2} = -2.28 \times 10^{-2} \text{ GeV}^3 (\pm 239\%). \end{aligned}$$

These three LDMEs are unphysically determined, which is reflected by the large relative errors shown in the end of each expressions. Nevertheless, it does not matter because we can find some linear combinations of them, which are physically determined and have small uncertainties. Define the correlation matrix C

$$C_{ij}^{-1} = \frac{1}{2} \frac{d^2 \chi^2}{dO_i dO_j}, \quad (9)$$

at the central value points, we have

$$C = \begin{pmatrix} 0.041 & -0.0060 & -0.011 \\ -0.0060 & 0.00087 & 0.0016 \\ -0.011 & 0.0016 & 0.0030 \end{pmatrix}. \quad (10)$$

The eigenvalues λ_i with corresponding eigenvectors $\vec{\nabla}_i$ of C are then

$$\begin{aligned} \lambda_1 &= 4.5 \times 10^{-2}, \quad \vec{\nabla}_1 = (0.96, -0.14, -0.26) \\ \lambda_2 &= 1.2 \times 10^{-6}, \quad \vec{\nabla}_2 = (0.29, 0.31, 0.91) \\ \lambda_3 &= 9.2 \times 10^{-9}, \quad \vec{\nabla}_3 = (0.047, 0.94, -0.33). \end{aligned} \quad (11)$$

The LDMEs corresponding to the eigenvectors are

$$\begin{pmatrix} \Lambda_1 \\ \Lambda_2 \\ \Lambda_3 \end{pmatrix} = V \begin{pmatrix} O_1 \\ O_2 \\ O_3 \end{pmatrix}, \quad (12)$$

where we denote matrix

$$V = \begin{pmatrix} \vec{\nabla}_1 \\ \vec{\nabla}_2 \\ \vec{\nabla}_3 \end{pmatrix}. \quad (13)$$

Inserting Eqs.(8) and (11) into Eq.(12), we have

$$\begin{aligned} \Lambda_1 &= 15.8 \times 10^{-2} \text{ GeV}^3 \quad (\pm 134\%), \\ \Lambda_2 &= 2.11 \times 10^{-2} \text{ GeV}^3 \quad (\pm 5.13\%), \\ \Lambda_3 &= 0.39 \times 10^{-2} \text{ GeV}^3 \quad (\pm 2.45\%). \end{aligned} \quad (14)$$

It can be seen that Λ_2 and Λ_3 are well constrained in this fit, while Λ_1 is badly determined which contains all unphysical information in Eq.(8). Using Λ_i , the differential cross section can be expressed as

$$d\sigma = \sum_{i=1}^3 d\hat{\sigma}_i O_i = \sum_{i=1}^3 a_i \Lambda_i, \quad \text{with } \vec{a} = d\vec{\sigma} V^{-1}, \quad (15)$$

where $d\hat{\sigma}_i$ denote the corresponding short-distance coefficients. With its large value and large uncertainty, Λ_1 may damage the theoretical results if its coefficient a_1 is not very small. Fortunately, with the CDF condition, we find contributions of Λ_1 , $\frac{a_1 \Lambda_1}{d\sigma}$, are less than four percent for all regions of $7 \text{ GeV} < p_T < 20 \text{ GeV}$.

In the above treatment, the LDMEs defined in Eq.(2) correspond to vectors $\vec{\nabla}_{M_0} = (0.25, 0, 0.97)$ and $\vec{\nabla}_{M_1} = (0, 0.87, -0.48)$, where we have normalized the vectors. We find $\vec{\nabla}_{M_0} \approx \vec{\nabla}_2$ and $\vec{\nabla}_{M_1} \approx \vec{\nabla}_3$. It means $M_{0,r_0}^{J/\psi}$ and $M_{1,r_1}^{J/\psi}$ are approximately equivalent to the two well constrained ones Λ_2 and Λ_3 respectively. As a result, if the badly determined Λ_1 is not important, results of using two LDMEs ($M_{0,r_0}^{J/\psi}$ and $M_{1,r_1}^{J/\psi}$) and using three LDMEs (Λ_1 , Λ_2 and Λ_3) should be approximately the same.

Comparisons of predictions between using two LDMEs and using three LDMEs are shown in Fig.4 and Fig.5 for the measured CMS[34] and LHCb[35] data respectively.

For the CMS condition ($\sqrt{S} = 7 \text{ TeV}$ and $|y_{J/\psi}| < 2.4$), we find from Fig.4 that the two methods give almost indistinguishable central values and error bars. This is understood as $r_{0,1}$ for CMS only have small differences from that for CDF, where the LDMEs are extracted. In this case, a_1 in Eq. (15) is much smaller than a_2 and a_3 , therefore the contribution of Λ_1 is ignorable although it has large uncertainty. We find that the theoretical predictions are in good agreement with the CMS data in a very wide range of p_T .

For the LHCb condition ($\sqrt{S} = 7 \text{ TeV}$ and $2.5 < y_{J/\psi} < 4$), we find from Fig.5 that although the two methods give the same central values, the method using three LDMEs have larger errors when $p_T > 9 \text{ GeV}$. The reason is the influence of a relatively large difference of r_1 between LHCb and CDF (about 18%) on the uncertainty in the method of using three LDMEs is enhanced by the large error of Λ_1 . On the other hand, the relatively large difference of r_1 may give a chance to extract

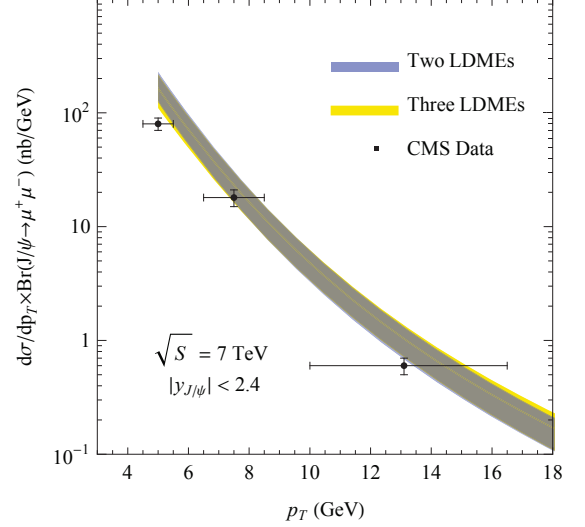


FIG. 4: (Color online.) Transverse momentum distributions of prompt J/ψ production at the LHC compared with the CMS data for $\sqrt{S} = 7 \text{ TeV}$ and $|y_{J/\psi}| < 2.4$. The CMS data are taken from Ref.[34]. The two methods give almost the same predictions.

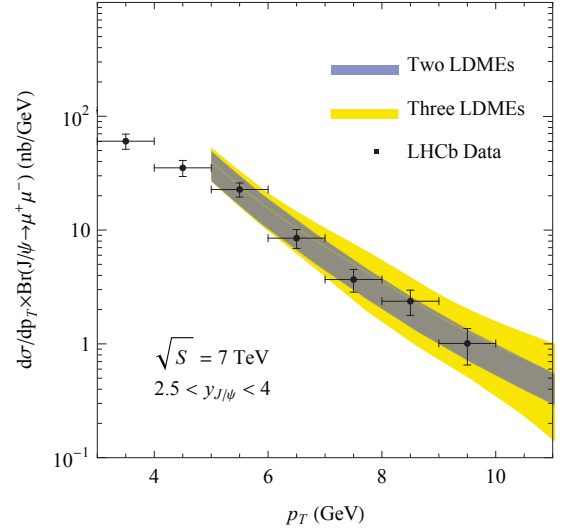


FIG. 5: (Color online.) Transverse momentum distributions of prompt J/ψ production at the LHC compared with the LHCb data for $\sqrt{S} = 7 \text{ TeV}$ and $2.5 < y_{J/\psi} < 4$. The LHCb data are taken from Ref.[35]. The two methods give the same predictions for the central values.

all three LDMEs with small uncertainties when experimental data at LHCb are adequate enough. Anyway, it can be seen from Fig.5 that our predictions give a good description for the LHCb data.

In short, the methods of using two LDMEs and using three LDMEs are consistent in giving predictions

in the present situation, when only two independent LDMEs can be well constrained. The method of using two LDMEs have advantages of simple formalism and intuitive physical implication, as they approximately represent the p_T^{-6} (for $M_{0,r_0}^{J/\psi}$) and p_T^{-4} (for $M_{1,r_1}^{J/\psi}$) behaviors of the cross section, but it needs to consider uncertainties originated from the decomposition Eq.(1) and the differences of $r_{0,1}$ additionally. On the other hand, the method of using three LDMEs can systematically treat all uncertainties but with a more complicated form, with which it may not be easy to see the physical meaning directly.

Within the method of using two LDMEs, whether a good prediction can be achieved is under control from the differences of $r_{0,1}$ between conditions under which we make predictions and conditions on which the LDMEs are extracted. Because the decomposition in Eq.(1) is good in the cases discussed in this work (see Table I), we expect there is no large uncertainty from it.

IV. PREDICTIONS FOR LHC AND RHIC

We compare our predictions of J/ψ prompt production at the LHC with new LHC data in Fig.6. The data of ALICE, ATLAS and LHCb Collaborations are taken from a recent meeting at CERN [36], while data of CMS Collaboration are taken from Ref. [37]. Besides statistical and systematic errors, comparable variations from spin-alignment uncertainty are also considered in data of ALICE, ATLAS and CMS Collaborations. Errors from spin-alignment are dominant for most p_T points, therefore, more studies on polarizations are needed in the future. On the theoretical side, we use the method of using two LDMEs as discussed in previous sections. It can be found that our predictions are in good agreement with all data on the whole. Specifically, from the comparison with the LHCb data, we find predicted cross sections become declining relative to data as $y_{J/\psi}$ becomes larger. This phenomenon, however, can be understood easily because r_1 tends to be far away from -0.56 when $y_{J/\psi}$ becomes larger (see Table I). On the other hand, as mentioned in the last section, the relative large difference of r_1 may give a chance to extract all three LDMEs when LHCb has enough data.

Data at large p_T are very important because they may distinguish between different models. Recently, both ATLAS[38] and CMS[39] Collaborations have released their data of prompt J/ψ production for p_T as large as 70 GeV. Comparisons with our predictions (with the same input parameters as in Refs.[1, 17]) are shown in Fig.7, where it is found that all data are located within predicted uncertainty bound (a factor of two). We fit the CO LDMEs using the Tevatron data with $7 \text{ GeV} < p_T < 20 \text{ GeV}$ and give a very good prediction for the LHC data up to $p_T = 70 \text{ GeV}$. This is a nontrivial test for the universality of CO LDMEs. Note that it is certainly needed to extract the CO LDMEs from these

large p_T data when data are adequate enough.

Our predictions for ψ' prompt production at the LHC compared with CMS data[39] and LHCb data[40] are shown in Fig.8. The predictions are in good agreement with CMS data. For the LHCb, because the data include also B decay contributions, we can not compare with them directly, but a consistence between data and prediction can still be found.

We also give predictions for J/ψ and ψ' productions at RHIC in Fig.9. It is found that the predictions are in good agreement with the data.

V. COMPARISON WITH RELATED WORK

Soon after this work was presented in a meeting[1], another talk[42] (see also [43]) appeared, in which a full NLO QCD correction to direct J/ψ production was also reported. They did not consider feeddown contributions of $\psi(2S)$ and χ_{cJ} to J/ψ production, but jointly fit the Tevatron data and HERA data for J/ψ production (Tevatron data with $p_T^{\text{cut}} = 3 \text{ GeV}$ and HERA data with $p_T^{\text{cut}} = 1 \text{ GeV}$). It is encouraging that, for all short-distance coefficients in J/ψ direct production at the Tevatron, results in our two groups consistent with each other.

However, the results of extracted LDMEs are significantly different. Specifically, they get [42]

$$\begin{aligned} \langle \mathcal{O}^{J/\psi}({}^1S_0^{[8]}) \rangle &= (4.76 \pm 0.71) \times 10^{-2} \text{ GeV}^3, \\ \langle \mathcal{O}^{J/\psi}({}^3S_1^{[8]}) \rangle &= (0.265 \pm 0.091) \times 10^{-2} \text{ GeV}^3, \\ \langle \mathcal{O}^{J/\psi}({}^3P_0^{[8]}) \rangle &= (-1.32 \pm 0.35) \times 10^{-2} \text{ GeV}^5. \end{aligned} \quad (16)$$

Inserting them into Eq.(1), we get

$$\begin{aligned} M_{0,r_0}^{J/\psi} &= 2.47 \times 10^{-2} \text{ GeV}^3, \\ M_{1,r_1}^{J/\psi} &= 0.594 \times 10^{-2} \text{ GeV}^3, \end{aligned} \quad (17)$$

which are much different from our results in Table II. The authors of Ref.[42] also pointed out that $M_{0,r_0}^{J/\psi}$ and $M_{1,r_1}^{J/\psi}$ are not precisely corresponding to the well constrained eigenvectors $\vec{\nabla}_2$ and $\vec{\nabla}_3$ in Eq.(11), but also mixed with $\vec{\nabla}_1$, thus in our fit there are very large uncertainties in LDMEs.

First of all, we note that a small mixing with $\vec{\nabla}_1$ is not so terrible. If we can expect that the physical LDME corresponding to $\vec{\nabla}_1$ is not much larger than that corresponding to $\vec{\nabla}_2$ and $\vec{\nabla}_3$, then the error caused by the mixing is just as large as the size of mixing, a few percents in our case. When the decomposition of Eq. 1 holds very well, there will be a LDME which can only be badly constrained. The fitted value of a badly constrained LDME is always much larger than its real value because of stochastic effect, which explains the fact that LDME corresponding to $\vec{\nabla}_1$ is much larger than that corresponding to $\vec{\nabla}_2$ and $\vec{\nabla}_3$ in Eq. 14.

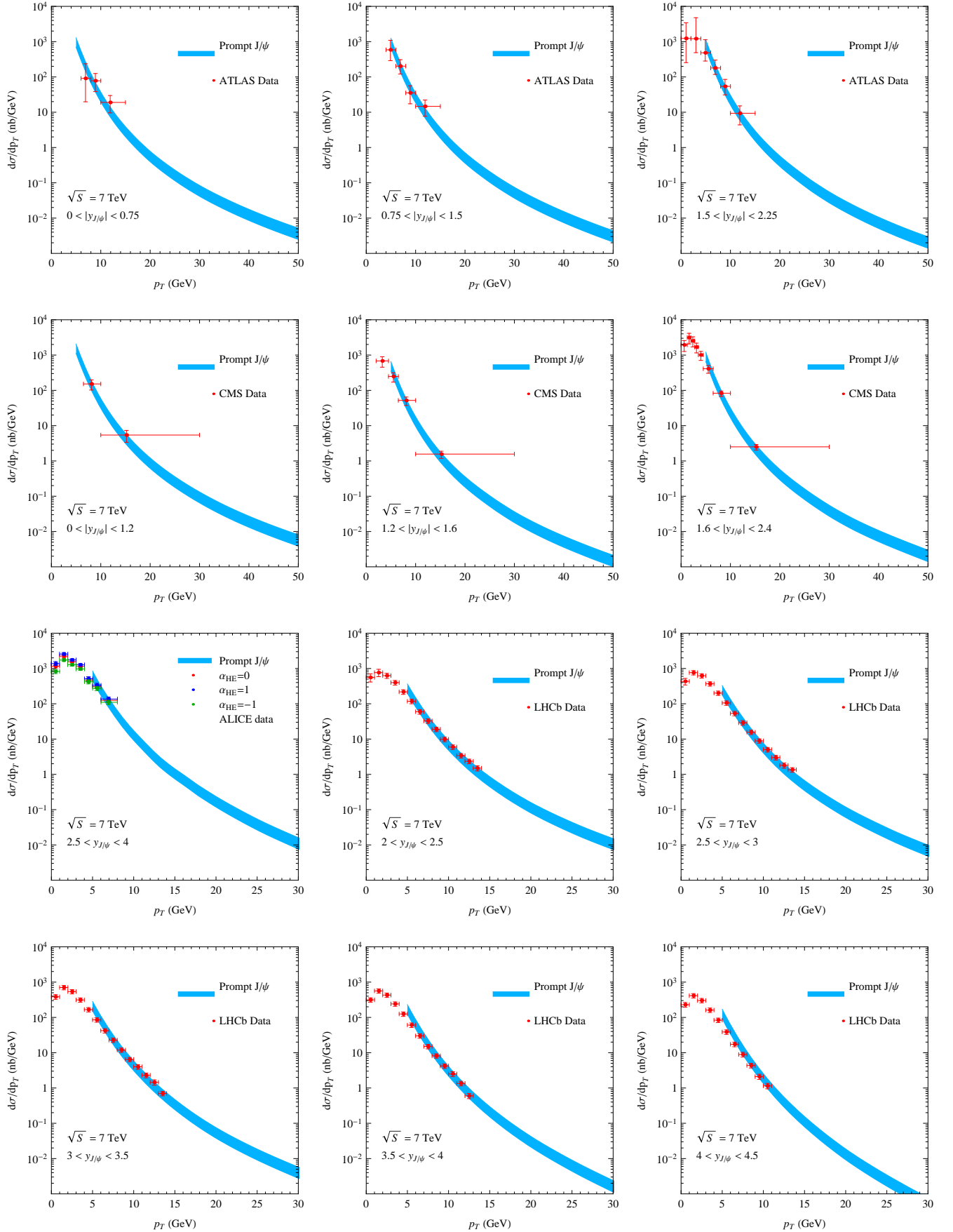


FIG. 6: (Color online.) Transverse momentum distributions of prompt J/ψ production at the LHC compared with the new data of ALICE, ATLAS, CMS and LHCb Collaborations for $\sqrt{S} = 7$ TeV. The LHC data are taken from Ref.[36, 37].

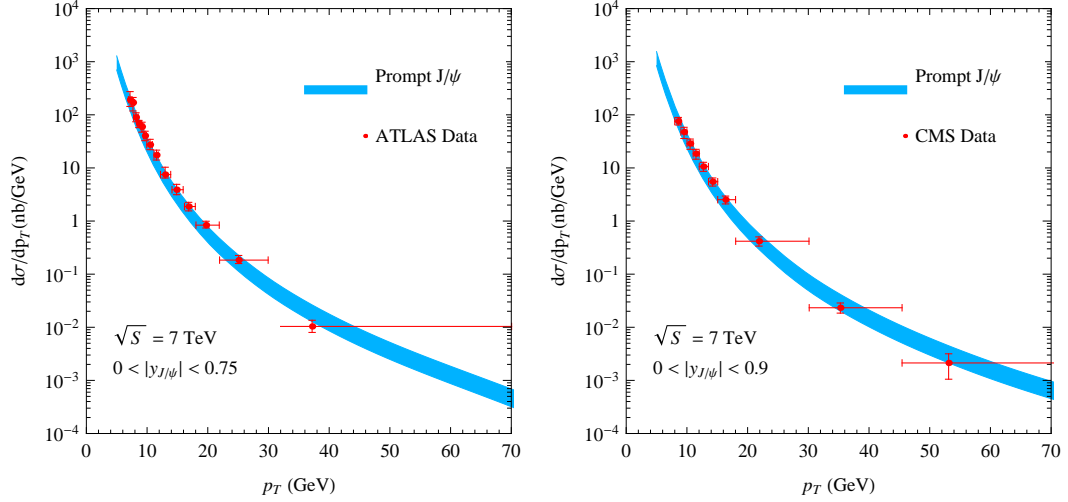


FIG. 7: (Color online.) Transverse momentum distributions of prompt J/ψ production at the LHC in large p_T region. The ATLAS data are taken from Ref.[38], and CMS data are taken from Ref.[39]

To clarify the discrepancy between Eq. 17 and Table II, we do a similar fit as authors in Ref. [42] did: using three LDMEs to fit the Tevatron data with $p_T^{\text{cut}} = 7$ GeV without considering feeddown contributions. We then get

$$\begin{aligned} M_{0,r_0}^{J/\psi} &= 8.54 \times 10^{-2} \text{ GeV}^3 \quad (\pm 12\%), \\ M_{1,r_1}^{J/\psi} &= 0.167 \times 10^{-2} \text{ GeV}^3 \quad (\pm 63\%). \end{aligned} \quad (18)$$

Comparing this result with that using two LDMEs to do the fit without considering feeddown contributions

$$\begin{aligned} M_{0,r_0}^{J/\psi} &= 8.92 \times 10^{-2} \text{ GeV}^3 \quad (\pm 4.4\%), \\ M_{1,r_1}^{J/\psi} &= 0.126 \times 10^{-2} \text{ GeV}^3 \quad (\pm 18\%), \end{aligned} \quad (19)$$

we find the two methods give very similar $M_{0,r_0}^{J/\psi}$ and $M_{1,r_1}^{J/\psi}$. Comparing Eq.(19) with Table II, we find the feeddown contributions change $M_{0,r_0}^{J/\psi}$ a little but reduce $M_{1,r_1}^{J/\psi}$ by a factor of 2.

We conclude that, even without subtracting feeddown contributions, results of only fitting Tevatron data with $p_T^{\text{cut}} = 7$ GeV in Eq.(18) are still significantly different from that in Eq.(17). Specifically, $M_{0,r_0}^{J/\psi}$ is well constrained in both Eq.(17) and Eq.(18), but the central value is much different. The difference, as short-distance coefficients are the same and the same fit method is used, must be ascribed to different treatments for experimental data in the fits. In our opinion, data for $p_T > 3$ GeV at the Tevatron and $p_T > 1$ GeV at HERA can not be described consistently by the fixed order perturbative NRQCD. The inconsistency may imply that the fixed order perturbative calculation can not describe the data in small p_T region ($3 \text{ GeV} < p_T < 7 \text{ GeV}$ for Tevatron and $p_T \sim 1 \text{ GeV}$ for HERA).

Besides, it will be interesting to see if the result given in Refs.[42, 43] can describe the large p_T J/ψ production

cross sections (say $20 \text{ GeV} < p_T < 70 \text{ GeV}$) observed very recently at the LHC, since the large p_T data provide a very important test for the LDMEs.

VI. SUMMARY

In summary, in this work we calculate the J/ψ and ψ' prompt production at the Tevatron, LHC, and RHIC at $\mathcal{O}(\alpha_s^4 v^4)$, including all CS, CO, and feeddown contributions. A large K factor of P-wave CO channels at high p_T results in two linearly combined LDMEs $M_{0,r_0}^{J/\psi}$ and $M_{1,r_1}^{J/\psi}$, which can be extracted at NLO from the Tevatron data. We argue that NLO result is necessary and essential to give a good description for J/ψ production, because the NNLO CS contributions are unlikely to be so important as to substantially enhance the cross sections at large p_T . We also compare the method of using two LDMEs with that using three LDMEs, and find these two methods can give consistent predictions in the present situation. For $r_{0,1}$, which appear in two combinations of LDMEs and are related to the short-distance coefficients depending on given experimental conditions (e.g., the beam energy, the rapidity values,...), when the differences of $r_{0,1}$ between the experiment in which the LDMEs are extracted, and the experiment for which the prediction is made, are small, the two methods give almost the same predictions with only small errors. Whereas when the differences are large, predictions of both of the two methods will have large uncertainties. Our theoretical predictions are in good agreement with the newly measured LHC data and RHIC data for both J/ψ and ψ' prompt production, which implies that the universality of CO LDMEs may hold approximately in charmonium hadroproduction. However, if one uses fixed order per-

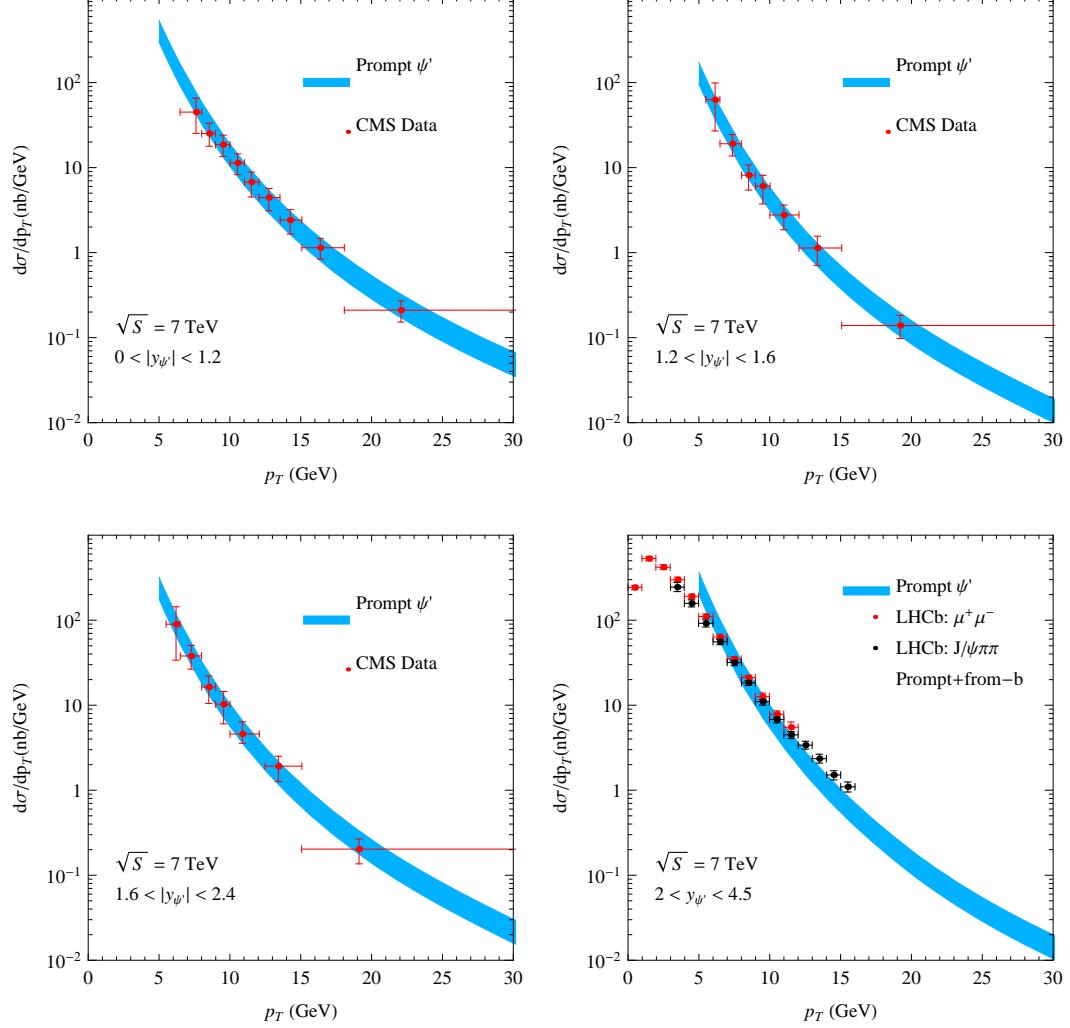


FIG. 8: (Color online.) Transverse momentum distributions of prompt ψ' production at the LHC. The CMS data are taken from Ref.[39], and LHCb data are taken from Ref.[40]. The LHCb data include also B decay contribution.

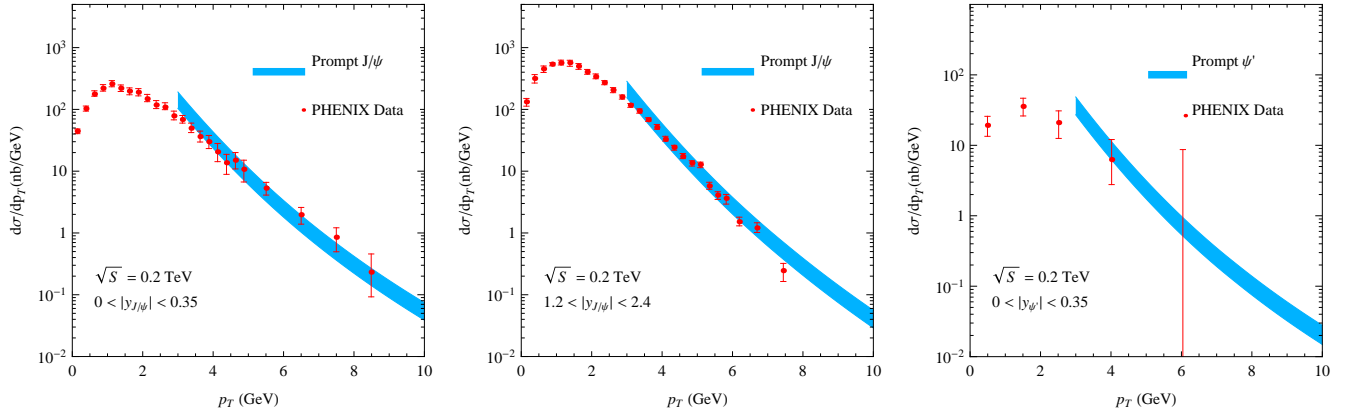


FIG. 9: (Color online.) Transverse momentum distributions of prompt J/ψ and ψ' production at RHIC. The PHENIX data are taken from Ref.[41]

turbative calculation to describe data in the small p_T region, we find the universality of color-octet matrix elements may be broken. Our work provides a new test for the universality of color-octet matrix elements, and the color-octet mechanism in general.

Acknowledgments

We thank G. Bodwin for helpful discussions and suggestions concerning the error analysis of using three

LDMes. Y. Q. Ma would also like to thank E. Braaten for useful comments when part of this result was reported at Topical Seminar on Frontier of Particle Physics 2010: Charm and Charmonium Physics, Beijing, China, August 27-31, 2010. This work was supported by the National Natural Science Foundation of China (No.10721063) and the Ministry of Science and Technology of China (No.2009CB825200).

-
- [1] Y. Q. Ma, talk presented at *Topical Seminar on Frontier of Particle Physics 2010: Charm and Charmonium Physics*, Beijing, China, August 27-31, 2010. URL: <http://bes3.ihep.ac.cn/conference/2010summersch/>.
 - [2] F. Abe *et al.* [CDF Collaboration], Phys. Rev. Lett. **69**, 3704 (1992).
 - [3] E. Braaten and S. Fleming, Phys. Rev. Lett. **74**, 3327 (1995) [arXiv:hep-ph/9411365].
 - [4] G. T. Bodwin, E. Braaten and G. P. Lepage, Phys. Rev. D **51**, 1125 (1995), D **55**, 5853 (E) (1997) [arXiv:hep-ph/9407339].
 - [5] M. Krämer, Prog. Part. Nucl. Phys. **47**, 141 (2001) [arXiv:hep-ph/0106120].
 - [6] N. Brambilla *et al.*, Eur. Phys. J. C **71**, 1534 (2011) [arXiv:1010.5827 [hep-ph]].
 - [7] A. A. Affolder *et al.* [CDF Collaboration], Phys. Rev. Lett. **85**, 2886 (2000) [arXiv:hep-ex/0004027]. A. Abulencia *et al.* [CDF Collaboration], Phys. Rev. Lett. **99**, 132001 (2007) [arXiv:0704.0638].
 - [8] For most recent study, see H. S. Chung, S. Kim, J. Lee and C. Yu, Phys. Rev. D **83**, 037501 (2011) [arXiv:1012.1954 [hep-ph]].
 - [9] P. Artoisenet, J. P. Lansberg and F. Maltoni, Phys. Lett. B **653**, 60 (2007) [arXiv:hep-ph/0703129].
 - [10] Z. G. He, R. Li and J. X. Wang, Phys. Rev. D **79**, 094003 (2009) [arXiv:0904.2069].
 - [11] Y. Fan, Y. Q. Ma and K. T. Chao, Phys. Rev. D **79**, 114009 (2009) [arXiv:0904.4025 [hep-ph]].
 - [12] G. C. Nayak, J. W. Qiu and G. Sterman, Phys. Lett. B **613**, 45 (2005) [arXiv:hep-ph/0501235], Phys. Rev. D **72**, 114012 (2005) [arXiv:hep-ph/0509021].
 - [13] H. Haberzettl and J. P. Lansberg, Phys. Rev. Lett. **100**, 032006 (2008) [arXiv:0709.3471 [hep-ph]].
 - [14] J. M. Campbell, F. Maltoni and F. Tramontano, Phys. Rev. Lett. **98**, 252002 (2007) [arXiv:hep-ph/0703113].
 - [15] B. Gong and J. X. Wang, Phys. Rev. Lett. **100**, 232001 (2008) [arXiv:0802.3727]; Phys. Rev. D **77**, 054028 (2008) [arXiv:0805.2469].
 - [16] Y. Q. Ma, K. Wang and K. T. Chao, Phys. Rev. D **83**, 11503(R) (2011) [arXiv:1002.3987].
 - [17] Y. Q. Ma, K. Wang and K. T. Chao, Phys. Rev. Lett. **106**, 042002 (2011) [arXiv:1009.3655 [hep-ph]].
 - [18] B. Gong, X. Q. Li and J. X. Wang, Phys. Lett. B **673**, 197 (2009) [Erratum-ibid. **693**, 612 (2010)] [arXiv:0805.4751 [hep-ph]].
 - [19] P. Artoisenet, J. Campbell, J. P. Lansberg, F. Maltoni, F. Tramontano, Phys. Rev. Lett. **101**, 152001 (2008) [arXiv:0806.3282].
 - [20] J. P. Lansberg, Eur. Phys. J. C **61**, 693 (2009) [arXiv:0811.4005].
 - [21] E. Braaten, M. A. Doncheski, S. Fleming and M. L. Mangano, Phys. Lett. B **333**, 548 (1994).
 - [22] M. Klasen, B. A. Kniehl, L. N. Mihaila and M. Steinhauser, Phys. Rev. Lett. **89**, 032001 (2002) [arXiv:hep-ph/0112259].
 - [23] P. Artoisenet, J. M. Campbell, F. Maltoni and F. Tramontano, Phys. Rev. Lett. **102**, 142001 (2009) [arXiv:0901.4352].
 - [24] C. H. Chang, R. Li and J. X. Wang, Phys. Rev. D **80**, 034020 (2009) [arXiv:0901.4749].
 - [25] M. Butenschoen and B. A. Kniehl, Phys. Rev. Lett. **104**, 072001 (2010) [arXiv:0909.2798].
 - [26] Y. Q. Ma, Y. J. Zhang and K. T. Chao, Phys. Rev. Lett. **102**, 162002 (2009) [arXiv:0812.5106].
 - [27] B. Gong and J. X. Wang, Phys. Rev. Lett. **102**, 162003 (2009) [arXiv:0901.0117].
 - [28] Y. J. Zhang, Y. Q. Ma, K. Wang and K. T. Chao, Phys. Rev. D **81**, 034015 (2010) [arXiv:0911.2166 [hep-ph]].
 - [29] Y. J. Zhang and K. T. Chao, Phys. Rev. Lett. **98**, 092003 (2007) [arXiv:hep-ph/0611086].
 - [30] Li Gang, Song Mao, Zhang Ren-You, Ma Wen-Gan, Phys. Rev. D **83**, 014001 (2011) [arXiv:1012.3798 [hep-ph]]; Song Mao, Ma Wen-Gan, Li Gang, Zhang Ren-You, Guo Lei, JHEP **1102**, 071 (2011) [arXiv:1102.0398 [hep-ph]].
 - [31] T. Aaltonen *et al.* [CDF Collaboration], Phys. Rev. D **80**, 031103 (2009) [arXiv:0905.1982].
 - [32] D. E. Acosta *et al.* [CDF Collaboration], Phys. Rev. D **71**, 032001 (2005) [arXiv:hep-ex/0412071].
 - [33] See the B-T model in E. J. Eichten and C. Quigg, Phys. Rev. D **52**, 1726 (1995) [arXiv:hep-ph/9503356].
 - [34] N. Leonardo, Proc. Sci., **ICHEP2010** (2010) 207.
 - [35] G. Passaleva, Proc. Sci., **ICHEP2010** (2010) 213.
 - [36] Talks presented at *Charm and bottom quark production at the LHC*, CERN, 3 December 2010. URL: <http://indico.cern.ch/conferenceDisplay.py?confId=111524>.
 - [37] V. Khachatryan *et al.* [CMS Collaboration], Eur. Phys. J. C **71**, 1575 (2011). [arXiv:1011.4193 [hep-ex]].
 - [38] Zdenek Dolezal, talk presented at *Moriond QCD and High Energy Interactions*, La Thuile, March 20-27, 2011. URL: <http://moriond.in2p3.fr/QCD/2011/MorQCD11Prog.html>.
 - [39] Fabrizio Palla, talk presented at *Europhysics Conference on High-Energy Physics 2011*, Grenoble, Friday, July 22, 2011. URL: <http://eps-hep2011.eu/>.
 - [40] L. L. Gioi, [arXiv:1109.3398 [hep-ex]].

- [41] A. Adare *et al.* [PHENIX Collaboration],
[arXiv:1105.1966 [hep-ex]].
- [42] M. Butenschoen, B. A. Kniehl, AIP Conf. Proc. **1343**,
409 (2011) [arXiv:1011.5619 [hep-ph]].
- [43] M. Butenschoen and B. A. Kniehl, Phys. Rev. Lett. **106**,
022003 (2011) [arXiv:1009.5662 [hep-ph]].